Analysis of urinary metabolomic profiling for unstable angina pectoris disease based on nuclear magnetic resonance spectroscopy

Zhongfeng Li[1,2] †, Xinfeng Liu[1]†, Juan Wang[2]†, Jian Gao[2], Shuzhen Guo[2], Kuo Gao[2], Hongxue Man[1],Yingfeng Wang[1], Jianxin Chen[2], Wei Wang[2]**

[1] Department of Chemistry, Capital Normal University, Beijing 100048, China.

[2] Beijing University of Chinese Medicine, Beijing 100029, China.

*To whom correspondence should be addressed:

Jianxin Chen

Beijing University of Chinese Medicine,

No.11 Beisanhuandonglu, Chaoyang District,

Beijing 100029, China.

E-mail: cjx@bucm.edu.cn

Fax: +86-010-64286283; Tel: +86-010-64286508

Wei Wang

Beijing University of Chinese Medicine,

No.11 Beisanhuandonglu, Chaoyang District,

Beijing 100029, China.

E-mail: wangwei@bucm.edu.cn

Fax: +86-010-64286283; Tel: +86-010-64286508

†Zhongfeng Li, Xinfeng Liu and Juan Wang contributed equally to this work.

Abstract

^{1}H NMR-based urinary metabolic profiling is used for investigating the unstable angina pectoris (UAP) metabolic signatures, in order to find out candidate biomarkers to facilitate medical diagnosis. In this work, 27 urine samples from UAP patients and 20 healthy controls were used. The metabolic profiles of the samples were analyzed by multivariate statistics analysis, including PCA, PLS-DA and OPLS-DA. The PCA analysis exhibited slight separation with R2X of 0.681 and Q2 of 0.251, while the PLS-DA (R2X= 0.121, R2Y = 0.931, Q2= 0.661) and the OPLS-DA (R2X =0.121, R2Y= 0.931, Q2=0.653) demonstrated that the model had good performance. By OPLS-DA, 20 metabolites were identified. A diagnostic model was further constructed using the receiver-operator characteristic (ROC) curves (AUC = 0.953), which exhibited satisfying sensitivity of 92.6%, specificity of 90% and accuracy of 89.1%. The results demonstrated that the NMR-based metabolomics approach possessed good performance to identify diagnostic urinary biomarkers, providing new insights into metabolic process related to UAP.

Keywords: Unstable angina pectoris (UAP), Metabolomics, Urine, NMR

Introduction

Unstable angina pectoris (UAP), a common complication of coronary heart disease (CHD), which accounts for more than one million hospitalizations annually, has affected as many as one third of individuals before the age of 70 years and contributed to a major cause of mortality and morbidity in developed countries[1-4].

In clinical practice, the symptoms of patients, such as high levels of cholesterol, triglyceride-rich lipoprotein particles (mainly VLDL and LDL) and lower levels of cholesterol in HDL particles, are critically important in making the diagnosis of UAP [5]. The most prevalent method is the angiography which is a kind of invasive imaging technique[2]. However, the current clinical management of UAP depends on assessing risk rather than on definitive diagnosis.

The pathogenesis of many diseases is associated with metabolite abnormalities in metabolism of body fluids and tissues[6]. Metabonomics broadly aims to measure the global, dynamic metabolic response of living systems to biological stimuli or genetic manipulation[7]. It enables the differential assessment of the levels of a broad range of endogenous and exogenous molecules and has been considered to have a great impact on the investigation of physiological status, diagnosis of diseases, discovery of biomarkers, and identification of perturbed pathways due to disease or treatment [8, 9].

High-resolution NMR spectroscopy, a quantitative and non-destructive technique, is a robust and reliable analytical method with paramount reproducibility and repeatability[10-12]. A NMR-based metabolomic approach instituting a sensitive high-throughput molecular screening has already demonstrated promising results in diagnosing a variety of cardiovascular system disorders[13−17].

Urine is an excellent biological fluid for various medical studies due to its easy collection from patients of all ages, low cell and protein content, and rich chemical composition.[18-20] Urinary metabolomics has emerged as a powerful non-invasive tool for diagnosing and monitoring variety of human diseases [21-26]. In the present study, we attempted to determine the features in urinary metabolites of UAP patients and healthy controls. The differences in metabolite profiles are identified between the urine of UAP patients and that of healthy controls as a result of physiological and pathological variations. Further characterization and validation with large sample size might help establish their utility as biomarkers of clinical benefit.

Materials and methods

Clinical Participant

All study participants were given informed consent for the investigation, which was approved by the Ethical Committee of Beijing University of Chinese Medicine. The study included 27 unstable angina pectoris patients from the Affiliated Dongfang Hospital of Beijing University of Chinese Medicine between May 2010 and August 2011. Healthy control subjects were 20 volunteers derived from the medical examination center of the Affiliated Dongzhimen Hospital of Beijing University of Chinese Medicine. Detailed data about patients and controls were presented in Table 1.

(1) Inclusion, Exclusion, and Rejection Criteria

All selected patients were diagnosed and confirmed by coronary angiography. Diagnosis criteria of UAP refer to "Treatment guide of stable angina" (ACC/AHA, 2002) and "Diagnosis and treatment recommendations of unstable angina" (Chinese Society of

Cardiology, 2000).

Inclusion criteria of UAP patients are as follows: (1) aged 20–90years old, male or female; (2) meeting the unstable angina diagnostic criteria. Inclusion criteria of healthy people cases are as follows: aged 20–90 years old, gender should correspond with the inclusion of patients; examination results were normal. All hospitalized patients had signed informed consent voluntarily.

Excluded cases were patients who suffered from acute myocardial infarction, myocarditis, pericardial disease, cardiac neurosis, intercostal neuralgia, menopausal syndrome, or severe spondylosis; angina caused by rheumatic fever, syphilis, congenital coronary artery abnormalities, hypertrophic cardiomyopathy, aortic stenosis, or regurgitation; stroke, lung infection, nephritis, renal failure, urinary tract infections, rheumatism, severe arrhythmia, heart failure, cancer, and other primary and serious diseases of liver, kidney, and hematopoietic system. Pregnant or lactating women, patients with allergies or psychosis, were also excluded.

Rejection Criteria. Violation of inclusion criteria or meeting the exclusion criteria was removed; persons missing the clinical data and who could not be statistically analyzed were removed.

(2) Collections of Clinical Data

General information, history, past medical history, family history, personal history, and signs were collected within 24 hours after the patients were admitted. Details of information from traditional four diagnostic methods were also recorded. Collections of patient histories and information from traditional four diagnostic methods were determined by the relevant professionals. Specific requirements include having the

occupation qualification, attending physician or above, and having relevant clinical experience more than two years.

Urine sample collection and preparation

The urine sample was collected from all patients in the morning after fasting for at least 12 hours and put into ice-cooled vessel containing 1% sodium azide and promptly placed in a freezer ($-20°C$).Within 3 hours of collection, the urine samples were stored in a $-80°C$ freezer until urinalysis.

Urine samples were thawed only once in a biosafety fume hood , and were prepared by mixing 550 μl of urine with 55 μl of 1.5 mol/L deuterated phosphate buffer (NaH_2PO_4 and K_2HPO_4, including 0.1% TSP (sodium 3-(trimethylsilyl)propionate-2,2,3,3-d4), pH 7.47), adding D_2O up to 550 μl if the urine is not enough. The urine-buffer mixture was left to stand for 5 min at room temperature and then centrifuged at 10000 rpm at 4 ℃ for 10 min to remove suspending debris. The supernatant (550μl) was then transferred into a 5 mm NMR tube. TSP served as a chemical shift reference ($\delta 0.0$)，and D_2O provided a lock signal.

^{1}H NMR spectroscopic measurement of urine

The urine samples were analyzed at 298 K using a VARIAN VNMRS 600 MHz NMR spectrometer (Varian Inc, Palo Alto, Calif) operating at 600.042 MHz using a 5-mm inverse-proton (HX) triple resonance probe with z-axis gradient coil. NMR spectra of the urine samples were acquired using the standard sequence: one dimensional spectrum using the first increment of the NOESY pulse sequence ($RD–90°–t_1–90°–t_m–90°–ACQ$) with water suppression, which was achieved with an

irradiation on the water peak during the relaxation delay (RD = 2.0 s) and a mixing time

(t_m) of 100 ms, t_1 was set to 4 µs. The 90° pulse length was adjusted to approximately 10

µs, and 128 transients were collected into 64K data points for each spectrum with a

spectral width of 20 ppm. The FIDs were weighted by an exponential function with a 0.5

Hz line-broadening factor prior to Fourier transformation. Standard COSY, TOCSY,

HMBC and J-resolved spectra were also acquired for metabolite identification of the

selected urine samples.

All of the ^{1}H NMR spectra were corrected for phase and baseline distortions

manually by MestReNova7.1.0 (Mestrelab Research, Spain). The spectral region δ

9.0-0.5 for each urine sample was automatically data reduced to 1700 integral segments

of equal length (0.005 ppm). The area under the spectrum was then calculated for each

segmented region and expressed as an integral value. The regions of water resonance

(δ5.20-4.70) were removed to eliminate baseline effects of imperfect water signal. The

choice of an appropriate normalization method should consider several aspects. The

optimal normalization method should be chosen carefully after consideration of the data,

experimental design, statistical aims, and the balance of accuracy and precision

ascertained through the use of auxiliary information[27]. As the concentration of creatinine

exist a little difference between different clinical samples, the integral data of each

spectrum were normalized to a constant sum of all the integrals in a spectrum to reduce

any significant concentration difference between the samples and then exported to text

files for further multivariate statistical analysis.

Multivariate statistical analysis

The resulting integral data were imported into SIMCA-P+12.0 (Umetrics, Sweden)

for multivariate statistical analysis. An unsupervised principal component analysis (PCA) model was performed using a mean-centered approach and data were visualized by the principal component (PC) score plots to identify general trends and outliers. To improve the separation due to patients and to minimize other biological analytical variation, sample classes were modeled using the PLS-DA (partial least-squares discrimination analysis) and O-PLS-DA (orthogonal projection to latent structure with discriminant analysis) algorithm at a unit variance-scaled approach. R2 and Q2 values were used to assess the amount of variation represented by the principal components and robustness of the model, respectively. The validity of the models against overfitting was assessed by the parameters R^2X and R^2Y, and the predictive ability was described by Q^2. All models were cross-validated by permutation tests (permutation numbers 200) [28,29]. The variable importance in the projection (VIP) value and the correlation coefficient (r) were used to reflect the importance of the metabolites, In our study, A |r| value > 0.432(for degree of freedom=19) and a VIP value > 1 were a priori considered as the cutoff value for the statistical significance on the basis of the literature[28]. The loading plots and differential metabolite peaks were displayed as positive and negative signals to represent the corresponding changes of metabolites by means of a MATLAB script (downloaded from http://www.mathworks.com) with some in-house modifications and were color-coded with absolute values of coefficients (|r|). On the loading plot, positive signals correspond to those metabolites that had an increased concentration in the urine of patients with UAP. Conversely, a negative signal corresponds to those metabolites that had an increased concentration in the urine of healthy controls. The main metabolites responsible for class discrimination were also manually calculated by peak integration.

In addition, an independent samples T-test was used to detect significant differences in selected signals between the two groups by SPSS Statistics Base 17.0 (SPSS Inc, USA). p value less than 0.05 was considered to be statistically significant. Additionally, diagnostic model was constructed by the marker metabolites alone using linear discrimination analysis method. We used random forest clustering to interrogate the top 20 biomarkers with significant alterations in the patients as compared to the control from the web site (http://www.metaboanalyst.ca/). The classification performance (sensitivity and specificity) of the OPLS-DA model and the area under the curve (AUC) of ROC were also calculated from the respective Monte-Carlo cross validation (MCCV) prediction (http://www.roccet.ca/).

Results

^{1}H NMR Spectra of Urine Samples

Urine is the most readily available biological fluids and contains a large number of metabolites secreted by the kidney after a series of biochemical process, thus it can provide valuable bio-information on the organism's metabolism. The representative spectra for ^{1}H NMR analysis of urine samples from unstable angina pectoris (UAP) patients and healthy controls (HC) were shown in Figure 1. Resonance assignments were performed according to the existing literature [30–32] and in-house NMR database and further confirmed with analysis of the 2D NMR spectroscopy (COSY, TOCSY, HMBC and J-resolved spectra). The spectra were dominated by a number of metabolites, including several kinds of short-chain fatty acids such as 3-Hydroxybutyrate and 3-Hydroxyisovalerate, some organic acids such as indol-3-acetate, hippurate and

methylmalonate, some amino acids such as lysine, proline, glutamine and phenyalanine etc. And some waste metabolites such as trimethylamine-N-oxide (TMAO), formate, trimethylamine(TMA), creatinine, choline, N-methylnicotinamide and carnosine. The urinary profile of the UAP group was characterized by lower levels of creatinine, histidine, choline, N-methylnicotinamide and carnosine, and higher levels of lysine, indol-3-acetate, hippurate and aspartate.

Metabonomics Analysis of Urine Samples of UAP and HC

PCA was first performed to detect any group separations based on NMR signal variability and the score plot was obtained with the first two PCs presenting 41.4 % and 26.7% variance, respectively (Figure 2; R2X = 68.1%, Q2 =25.1%). Figure 2 showed a good trend of separation between UAP group and HC group along PC1, but there was also a partial overlap, so there was no significant difference between healthy controls and UAP patients according to the PCA score plot.

Then, a cross-validated PLS-DA model with satisfactory discriminating ability was established to assess the metabolic differences between UAP and HC (Figure 3). PLS-DA is a supervised method of data analysis which could maximize differences between groups and aid in the screening of the metabolite responsible for class separation by removing systematic variations unrelated to pathological status [16]. On the score plot of the PLS-DA model (Figure 3A), UAP patients and healthy controls were discriminated obviously with R2X = 12.1%, R2Y = 93.1%, and Q2 = 66.1%. The parameters for describing the PLS-DA model were significantly elevated (R2Y, Q2 > 0.5), suggesting that the PLS-DA model was robust. To validate the performance of the PLS-DA model, a 200-iteration permutation test was performed. The validation plot (Figure 3B)

demonstrated that the original PLS-DA model was not random and overfitting as both permutated Q2 and R2 values were significantly lower than the corresponding original values.

To eliminate the influence of individual difference and have an insight into the changed metabolites responsible for the separation between two groups, the OPLS-DA model was constructed using the first principal component and the second orthogonal component. The quality of model was described by the cross-validation parameters Q2Y, indicating the predictability of the model, and R2Y, representing the total explained variation for the matrix. In OPLS-DA score plot (R2Y=0.931, Q2Y=0.653), a significant biochemical distinction between the UAP patients and healthy controls was identified (Figure 4A). The metabolic changes in UAP patients were reflected in the color coded coefficient plot (Figure4B). Metabolites exhibiting significant changes (P < 0.05) were identified based on the absolute cutoff value of correlation coefficients (|r|) and VIP value and were listed in Table 2. With a |r| value > 0.432(for degree of freedom=19) and a VIP value >1, the urine samples of UAP patients showed up-regulation of lysine, indol-3-acetate, hippurate, aspartate and down-regulation of 3-hydroxybutyrate, methylmalonate, proline, glutamine, TMA, creatinine, cis-aconitate, citrulline, histidine, choline, tryptophan, phenylalanine, τ-methylhistidine, carnosine, N-methylnicotinamide, trigonelline.

In addition, the hierarchical cluster analysis (HCA) could readily be used to assess relatedness and distance of any type of samples characterized by any type of descriptors, and the result was displayed as 'heatmap'. We used the metabolites listed in Table 2 as

the variables to conduct the HCA, and got the heatmap(Figure 5). The heatmap showed that the UAP patients and healthy controls were almost completely separated from each other, as the change of the metabolites was similar in the same group, and different in the different group. It could be observed that the metabolic state of UAP patients resulted in the decreased urine levels of 3-hydroxybutyrate, methylmalonate, proline, glutamine, TMA, creatinine, cis-aconitate, citrulline, histidine, choline, tryptophan, phenylalanine, τ-methylhistidine, carnosine, N-methylnicotinamide and trigonelline, as well as elevated levels of lysine, indol-3-acetate, hippurate and aspartate. The result of HCA further illustrated that these metabolites could distinguish the UAP patients and healthy controls, so these endogenous metabolites could be used as the potential biomarkers.

Prediction and diagnostic performance test

To validate the proposed OPLS-DA model and test its applicability in diagnosing UAP, ROC curves analysis was performed to validate the clinical efficacy of these potential biomarkers. Areas under the ROC curve (AUC) were generally considered as the method of choice for evaluating the performance of potential biomarkers: the greater the AUC, the better the prediction of the model. **Figure 6A** showed a set of ROC curves for SVM models created using different subsets of metabolites selected by the filter approach, six models were developed. The top 2 important variables (choline and N-methylnicotinamide) were used to build classification models, the AUC value was 0.82 and 95% confidence interval (CI) was 0.665-0.947. The AUC using a larger number of variables achieved even greater areas under the ROC curves, and got the maximum value 0.953 (95%CI, 0.849-1) when we used 18 metabolites as the variables. Meanwhile, the predictive accuracy was the maximum value 89.1% (**Figure 6B**). The metabolites in

Figure 6C were ranked by their contribution to distinguishing the UAP from controls. The greater the distance from the Y-axis, the greater the contribution of a particular metabolite in distinguishing cases from controls. This plot also indicated whether the metabolite concentration was increased or decreased in cases related to controls. The 18 metabolites in **Figure 6C** include choline, N-methylnicotinamide, citrulline, trimethylamine, creatinine, carnosine, aspartate, tryptophan, trigonelline, cis-aconitate, indol-3-acetate, hippurate, 3-hydroxybutyrate, glutamine, lysine, methylmalonate, τ-methylhistidine and phenylalanine, and the importance decreased in this order. The predicted class probabilities (average of the cross-validation) for each sample using the best classifier (based on AUC) is illustrated in **Figure 6D**. The verification results showed that in the 27 UAP samples, 25 were predicted correctly, and in the 20 healthy control samples, 19 correctly. Therefore, the OPLS-DA prediction model exhibited a sensitivity of 92.6% and a specificity of 90% for UAP diagnosis. On the basis of selected biomarkers, ROC analysis revealed that UAP not only generate signature biomarkers and that these biomarkers can be used to diagnose them.

Metabolic Pathway and Function Analysis

In addition, based on the identified biomarkers, the urine metabolic pathway analysis was performed using MetPA to reveal the most relevant pathways related to UAP. The impact value of these pathways calculated from pathway topology analysis above 0.1 was screened out as potential target pathway. According to the impact value, we finally found 7 potential target pathways related to 12 metabolites indentified in this research. The 5 pathways (aminoacyl-tRNA biosynthesis, arginine and proline metabolism, histidine metabolism, alanine, aspartate and glutamate metabolism   and

phenylalanine metabolism) , which included more than one target, were disturbed when UAP occurred (Figure 7). The details of pathways were displayed in supplementary Table S1 and Figure S1-5, Supporting Information.

Discussion

Unstable angina pectoris (UAP) involves the sense of chest pain, pressure, or squeezing, often due to ischemia of the heart muscle from obstruction or spasm of the coronary arteries and it had been a great threat to the human health. The UAP can be controlled well when the diagnosis is timely, accurate, and definitive. Although humoral markers of plaque vulnerability [C-reactive protein; interleukin (IL)-6, IL-10 and IL-18 and CD-40L] had been identified, these markers were of limited clinical use for diagnosis and risk stratification in individual patients. However, it should be noted that the metabolic state of the heart was at least partly reflected in urine metabolites that clearly pointed to an altered energy metabolism in UAP patients, which could be harnessed as markers of disease. Further mechanistic studies regarding this issue were warranted.

In the present study, a ^{1}H NMR-based metabonomic approach was employed to demonstrate metabolic differences between UAP patients and healthy controls. Subsequent analysis of the metabolite profiles of urine samples from UAP patients could distinguish patients from healthy normal controls and provide a fingerprint of metabolic changes that characterized the disease, and highlighted the potential of metabolomic analysis in the evaluation of a disease condition. Moreover, this approach was used to assess its accuracy and reliability in diagnosing UAP, which showed better performance in terms of both specificity and sensitivity. The 20 key metabolites responsible for discrimination between UAP patients and healthy controls were identified. These

metabolites include energy metabolism-related molecules (creatinine, cis-aconitate, methylmalonate and 3-hydroxybutyrate), amino acids (glutamine, citrulline, tryptophan, phenylalanine, τ-methylhistidine, lysine and aspartate), and the other metabolism molecules (TMA, choline, carnosine, hippurate, trigonelline N-methylnicotinamide and indol-3-acetate). And the combination of 18 metabolites appeared to be highly accurate predictors of UAP status. The sensitivity of this combination of metabolites was 92.6% at a specificity threshold of 90%. In our study, seven unique metabolic pathway of aminoacyl-tRNA biosynthesis, arginine and proline metabolism, histidine metabolism, alanine, aspartate and glutamate metabolism, phenylalanine metabolism, lysine degradation and tryptophan metabolism were identified from UAP patients.

Creatinine is derived from creatine and phosphocreatine. The phosphagen system is very important for cellular energy transfer, and can be viewed as the body's energy buffer solution to maintain the balance of ATP in the body[34,35]. Under normal circumstances, most creatine transforms into phosphocreatine and generates ATP by the function of enzyme which process is reversible. In other cases it turns into creatinine without enzyme. The decreased level of urine creatinine in the UAP group illustrates that the UAP patients could not produce ATP normally, and need more creatine transformed into phosphocreatine to generate ATP[36]. Cis-aconitate is an important intermediate of TCA cycle, the decreased level may stem from the suppressed TCA cycle. The confusion of energy metabolism may come from the cardiac abnormality and insufficient oxygen supply to the body. Methylmalonate can transform into succinyl-CoA finally by the function of a series enzyme to get into TCA cycle. This is one of the anaplerotic reactions in the organism. Seok-Min Kang et al.[37] found that there was a perturbation in

methylmalonate metabolism in patients with ischemic HF. The changes in the concentrations of methylmalonate also show the confusion of Krebs cycle indirectly.

Glutamine is a kind of glucogenic amino acid, and it is also an important fuel for gluconeogenesis. The glutamine is the central part of the TCA cycle and plays an important role in many metabolic pathways, especially in maintaining the amino acid homeostasis. Turer et al [38] used metabolomic profiling to compare cardiac extraction and plasma substrates, and demonstrated that patients with CHD had decreased concentration of glutamate/glutamine. In this study, its reduced content maybe caused by the disorder of amino acid metabolism, Lysine can lower the levels of blood triglycerides to prevent cardiovascular and cerebrovascular disease, and its elevated content is the result of the organism self-adjustment. By the catalysis of enzyme, histidine could be transformed into histamine in the organism. The role of histamine is to dilate blood vessels and lower blood pressure. John et al[39] illustrated that histidine was an effective quencher of singlet oxygen and could significantly improve the functional recovery of ischemic myocardium, and the decreased level of histidine aggravates the disease. Aspartate can be used as the carrier of K^+, Mg^{2+} into myocardial areas by improving the myocardial systolic function and lowering oxygen consumption.

In the organism, PCho/Cho can regulate lipid metabolism, and the choline also can soften the cholesterol to prevent it from accumulating in the blood vessel walls. Choline deficiency is also associated with increased lipid accumulation[40]. The decreased level of choline is not conducive to the recovery. 3-Hydroxybutyrate is a ketone body. In human body, 3-hydroxybutyrate can be used as an energy source by the brain when blood sugar is low. Ketone bodies serve as an indispensable source of energy for extrahepatic tissues,

especially the brain and lung of advanced mammals. Another important function of ketone bodies is to provide acetoacetyl-CoA and acetyl-CoA for synthesis of cholesterol, fatty acids, and complex lipids, so the 3-Hydroxybutyrate deficiency is helpful to the recovery.

Conclusion

In the present study, ^{1}H NMR-based metabolomics method combined with multivariate data analysis was used to distinguish independently UAP patients from healthy controls with high reliability. 20 potential biomarkers related to UAP disease were found by analysis and using 18 of the 20 metabolites as the biomarkers in diagnosing UAP disease exhibited a sensitivity of 92.6%, a specificity of 90% and an accuracy of 89.1%. The metabolomic approach is proved to be useful in improving the under diagnosis of UAP. However, compared with other new diagnostic approach, there are some limitations in our study attributed to the effects of other combinations on the metabolic profiles. This potential confounding factor can be analyzed by subgroups, and therefore, may be an interesting subject for further study.

Notes

The authors declare no competing financial interest.

Molecular BioSystems Accepted Manuscript

Supporting Information Available: Figure S1, the pathways of Aminoacyl-tRNA biosynthesis; Figure S2, the pathways of Arginine and proline metabolism; Figure S3, the pathways of Histidine metabolism; Figure S4, the pathways of Alanine, aspartate and glutamate metabolism; Figure S5, the pathways of Phenylalanine metabolism; Table S1, Results from Pathway Analysis with MetPA from urine. This material is available free of charge via the Internet at http://www.rsc.org.

References:

(1) A. Kibos and A. Guerchicoff, Susceptibility genes for coronary heart disease and myocardial infarction. *Acute Cardiac Care.* **2011**, 13 (3), 136–142.

(2) A. A. John, L. W. Stephen, S. Auderey, E. Angie and E. Louis, Angiographic Morphology and the Pathogenesis of Unstable Angina Pectoris. J*ournal of the American College of Cardiology,* **1985**, 5, 609–616.

(3) S. Allender, P. Scarborough, M. O'Flaherty and S. Capewell, 20th century CHD morality in England and Wales: population trends in CHD risk factors and coronary death. *BMC Public Health.* **2008**, 8, 148.

(4) B. Unal, J. A. Critchley and S. Capewell, Explaining the decline in coronary heart disease mortality in England and Wales between 1981 and 2000. *Circulation*. **2004**, 109, 1101-1107.

(5) C. Delles, E. Schiffer, C. von zur Muhlen, K. Peter, P. Rossing, H. Parving, J. A. Dymott, U. Neisius, L. U. Zimmerli, J. K. Snell-Bergeon, D. M. Maahs, R. E. Schmieder, H. Mischak and A. F. Dominiczak, Urinary proteomic diagnosis of coronary artery disease: identification and clinical validation in 623 individuals. Journal of Hypertension,   2010, 28 , 2316-2322

(6) C. E. Wheelock, A. M. Wheelock, S. Kawashima, D. Diez, M. Kanehisa and M. Erk, *et al,* Systems biology approaches and pathway tools for investigating cardiovascular disease , *Mol. BioSyst.*, 2009,5, 588-602

(7) J. K. Nicholson and J. C. Lindon, Systems biology: metabonomics. *Nature*. **2008**, 455 (7216), 1054.

(8) M. H. Abu Bakar, M. R. Sarmidi, K. K. Cheng, A. A. Khan and C. L. Suan, *et*

al., Metabolomics- the complementary field in systems biology: a review on obesity and type 2 diabetes , *Mol. BioSyst.,* 2015,11, 1742-1774

(9) G. Gowda, S. Zhang, H. Gu, V. Asiago, N. Shanaiah and D. Raftery, Metabolomics-based methods for early disease diagnostics. *Expert Rev. Mol. Diagn.* **2008**, 8 (5), 617 −633

(10) J. K. Nicholson and I. D. Wilson, High resolution proton magnetic resonance spectroscopy of biological fluids. *Prog. Nucl. Magn. Reson. Spectrosc.* **1989**, 21, 449–501.

(11) J. Y. Jung, H. S. Lee, D. G. Kang, N. S. Kim, M. H. Cha, O. S. Bang, H. Ryu do and G. S. Hwang, ^{1}H-NMR-Based Metabolomics Study of Cerebral Infarction. *Stroke.* **2011**, 42 (5), 1282 −1288.

(12) A. Sussulini, A. Prando, D. A. Maretto, R. J. Poppi, L. Tasic, C. E. Banzato and M. A. Arruda, Metabolic profiling of human blood serum from treated patients with bipolar disorder employing ^{1}H NMR spectroscopy and chemometrics. *Anal. Chem.* **2009**, 81 (23), 9755 −9763.

(13) P. Bernini, I. Bertini, C. Luchinat, L. Tenori and A. Tognaccini, The Cardiovascular Risk of Healthy Individuals Studied by NMR Metabonomics of Plasma Samples. J. Proteome Res. **2011**, 10, 4983-4992.

(14) J. T. Brindle, J. K. Nicholson, P. M. Schofield, D. J. Grainger and E. Holmes, Application of chemometrics to ^{1}H NMR spectroscopic data to investigate a relationship between human serum metabolic profiles and hypertension. *Analyst.* **2003**, 128, 32–36.

(15) G. J. Blake, J. D. Otvos, N. Rifai and P. M. Ridker, Low-density lipoprotein particle

concentration and size as determined by nuclear magnetic resonance spectroscopy as predictors of cardiovascular disease in women. *Circulation*. **2002**, 106, 1930–1937.

(16) R. Amathieu, P. Nahon, M. Triba, N. Bouchemal, J. C. Trinchet, M. Beaugrand, G. Dhonneur and L. Le Moyec, Metabolomic approach by ^{1}H NMR spectroscopy of serum for the assessment of chronic liver failure in patients with cirrhosis. *J. Proteome Res*. **2011**, 10, 3239-3245.

(17) J. T. Brindle, H. Antti, E. Holmes, G. Tranter, J. K. Nicholson, H. W. L. Bethel, S. Clarke, P. M. Schofield, E. McKilligin, D. E. Mosedale and D. J. Grainger, Rapid and noninvasive diagnosis of the presence and severity of coronary heart disease using ^{1}HNMR-based metabonomics. *Nature*. Med. **2002**, 8, 1439–1444.

(18) H. J. Issaq, O. Nativ, T. Waybright, B. Luke, T. D. Veenstra, E. J. Issaq, A. Kravstov and M. Mullerad, Detection of bladder cancer in human urine by metabolomic profiling using high performance liquid chromatography/mass spectrometry. *J. Urology*. **2008**, 179: 2422–2426.

(19) A. Pechlivanis, S. Kostidis, P. Saraslanidis, A. Petridou, G. Tsalis, V. Mougios, H. G. Gika, E. Mikros and G. A. Theodoridis, ^{1}H NMR-Based Metabonomic Investigation of the Effect of Two Different Exercise Sessions on the Metabolic Fingerprint of Human Urine. *J. Proteome Res*. **2010**, 9 (12), 6405–6416.

(20) K. B. Kim, S. Y. Um, M. W. Chung, S. C. Jung, J. S. Oh, S. H. Kim, H. S. Na, B. M. Lee and K. H. Choi, Toxico metabolomics approach to urinary biomarkers for mercuric chloride (HgCl)- induced nephrotoxicity using proton nuclear magnetic resonance ((1)H NMR) in rats. *Toxicol. Appl. Pharmacol*. **2010**, 249, 114–126.

(21) K. Kim, P. Aronov, S. O. Zakharkin, D. Anderson, B. Perroud, I. M. Thompson and

R. H. Weiss, Urine metabolomics analysis for kidney cancer detection and biomarker discovery. *Mol Cell Proteomics*. **2009**, 8, 558–570.

(22) K. K. Pasikanti, K. Esuvaranathan, P. C. Ho, R. Mahendran, R. Kamaraj, Q. H. Wu, E. Chiong and E. C. Y. Chan, Noninvasive urinary metabonomic diagnosis of human bladder cancer. *J. Proteome Res*. **2010**, 9, 2988–2995.

(23) S. M. Kang, J. C. Park, M. J. Shin, H. Lee and J. H. Oh, Nuclear magnetic resonance based metabolic urinary profiling of patients with ischemic heart failure. *Clin Biochem*. **2011**, 44: 293–299.

(24) U. F. Engelke, S. M. L. Liebrand-van, J. J. G. N. De, J. G. Leroy, E. Morava, J. A. M. Smeitink and R. A. Wevers, N-acetylated metabolites in urine: proton nuclear magnetic resonance spectroscopic study on patients with inborn errors of metabolism. *Clin Chem*. **2004**, 50, 58–66.

(25) E. J. Saude, C. D. Skappak, S. Regush, K. Cook, A. Ben-Zvi, A. Becker, R. Moqbel, B. D. Sykes, B. H. Rowe and D. J. Adamko, Metabolomic profiling of asthma: Diagnostic utility of urine nuclear magnetic resonance spectroscopy. *J. Allergy Clin Immun*. **2011**, 127 (3), 757–764.

(26) S. Bouatra, F. Aziat, R. Mandal, A. C. Guo, M. R. Wilson, C. Knox, T. C. Bjorndahl, R. Krishnamurthy, F. Saleem and P. Liu, The Human Urine Metabolome. *PLoS One*. **2013**, 8(9), e73076.

(27) A. M. De Livera, D. A. Dias, D. De Souza, T. Rupasinghe, J. Pyke, D. Tull, U. Roessner, M. McConville and T. P. Speed, Normalizing and Integrating Metabolomics Data. *Anal. Chem.* **2012**, 84, 10768−1077

(28) W. B. Dunn and D. I. Ellis, Metabolomics: current analytical platforms and

methodologies. *TrAC, Trends Anal. Chem*. **2005**, 24, 285-294.

(29) B M. ylesjoe, M. Rantalainen, O. Cloarec, J. K. Nicholson, E. Holmes and J. Trygg, OPLS discriminant analysis: combining the strengths of PLS-DA and SIMCA classification. *J. Chemom*. **2006**, 20, 341-351.

(30) W. J. Yang, Y. W. Wang, Q. F. Zhou and H. R. Tang, Analysis of human urine metabolites using SPE and NMR spectroscopy. *Sci China Ser B*. **2008**, 51(3), 218–225.

(31) B. Ross and T. Michaelis, Clinical application of magnetic resonance spectroscopy. *Magnetic Resonance Q*. **1994**, 10, 191–247.

(32) T. M. rupp, P. Jonsson, A. Oehrfelt, H. Zetterberg, O. Obudulu, L. Malm, A. Wuolikainen, J. Linder, T. Moritz and K. Blennow, Metabolite and peptide levels in plasma and CSF differentiating healthy controls from patients with newly diagnosed Parkinson's disease. *J. Parkinson's Dis*. **2014**, 4 (3), 549-560.

(33) Y. Liu, Z. B. Lin, G. G. Tan, Z. Y. Chu, Z. Y. Lou, J. P. Zhang, Z. Y. Hong and Y. F. Chai, Metabonomic studies on potential plasma biomarkers in rats exposed to ionizing radiation and the protective effects of Hong Shan Capsule. *Metabolomics.* **2013**, 9(5), 1082-1095.

(34) M. Wyss and R. Kaddurah-Daouk, Creatine and creatinine metabolism. *Physiological Reviews*. **2000**, 80, 1107–1213.

(35) Z. P. heng, H. C. Gao, Q. Li, W. H. Shao, M. L. Zhang, K. Cheng, D. Y. Yang, S. H. Fan, L. Chen, L. Fang and P. Xie, Plasma Metabonomics as a Novel Diagnostic Approach for Major Depressive Disorder. *J. Proteome Res*. **2012**, 11(3), 1741-1748.

(36) J. Carrola, C. M. Rocha, A. S. Barros, A. M. Gil, B. J. Goodfellow, I. M. Carreira, J. Bernardo, A. Gomes, V. Sousa, L. Carvalho and I. F. Duarte, Metabolic Signatures of Lung Cancer in Biofluids: NMR-Based Metabonomics of Urine. *J. Proteome Res*. **2011**, 10(1), 221-230.

(37) S. M. Kang, J. C. Park, M. J. Shin, H. Lee, J. Oh, H. Ryu do, G. S. Hwang and J. H. Chung, ^{1}H nuclear magnetic resonance based metabolic urinary profiling of patients with ischemic heart failure. *Clin Biochem Mar*. **2011**, 44 (4), 293-9.

(38) A. T. Turer, R. D. Stevens, J. R. Bain, M. J. Muehlbauer, W. J. van de, J. P. Mathew, D. A. Schwinn, D. D. Glower, C. B. Newgard and M. V. Podgoreanu, Metabolomic profiling reveals distinct patterns of myocardial substrate use in humans with coronary artery disease or left ventricular dysfunction during surgical ischemia/reperfusion. *American Heart Association*. **2009**, 119(13), 1736-1746.

(39) J. W. Lee, H. Miyawaki, E. V. Bobst, J. D. Hester, M. Ashraf and A. M. Bobst, Improved functional recovery of ischemic rat hearts due to singlet oxygen scavengers histidine and carnosine. *J. Mol Cell Cardiol*. **1999**, 31,113–121.

(40) C. Oakman, L. Tenor, L. Biganzoli, L. Santarpia, S. Cappadona, C. Luchinat and A. Di Leo, Uncovering the metabolomic fingerprint of breast cancer. *Int J Biochem and Cell Biol*. **2011**, 43, 1010-1020.
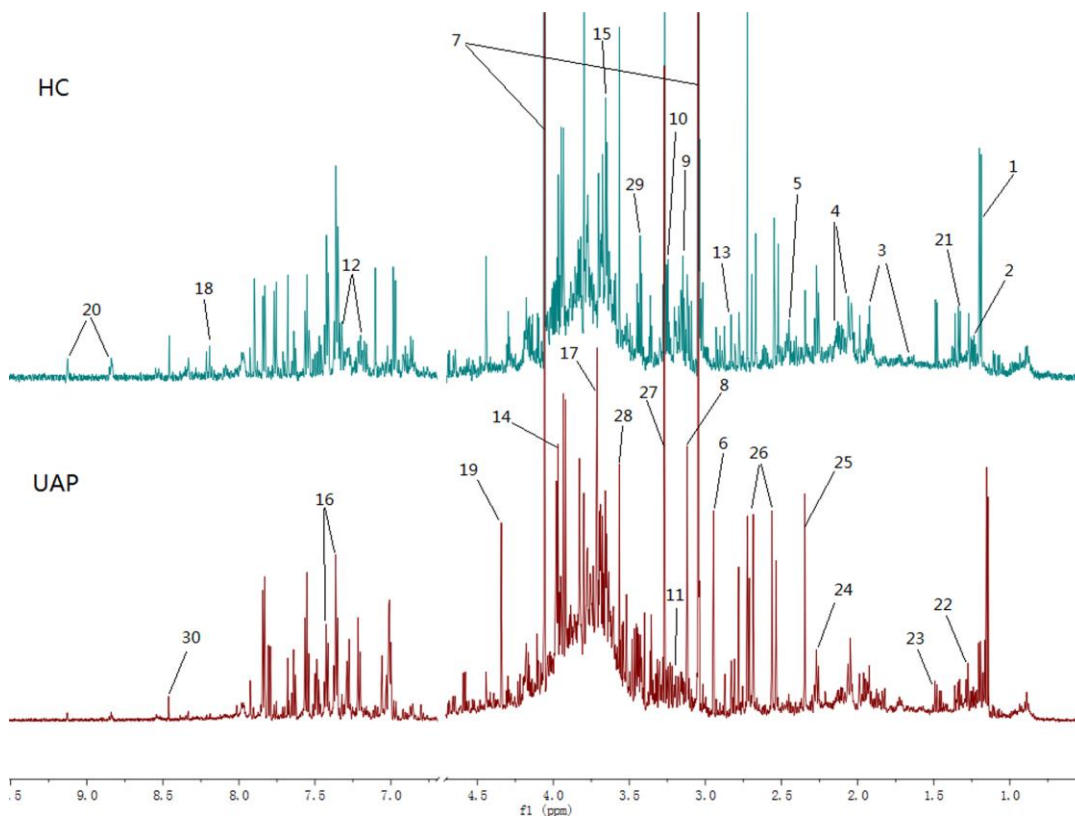
Figure 1. Representative 600 MHz ^{1}H NMR spectra of urine samples from UAP patient and healthy control subject, Distinguished metabolites: 1 3-hydroxybutyrate, 2 methylmalonate, 3 lysine, 4 proline, 5 glutamine, 6 trimethylamine, 7 creatinine, 8 cis-aconitate, 9 citrulline, 10 histidine, 11 choline, 12 tryptophan, 13 aspartate, 14 hippurate, 15 indol-3-acetate, 16 phenylalanine, 17 τ-methylhistidine, 18 carnosine, 19 N-methylnicotinamide, 20 trigonelline, 21 threonine, 22 3-hydroxyisovalerate, 23 alanine, 24 Acetoacetate, 25 succinate, 26 citrate, 27 TMAO, 28 glycine, 29 taurine, 30 formate
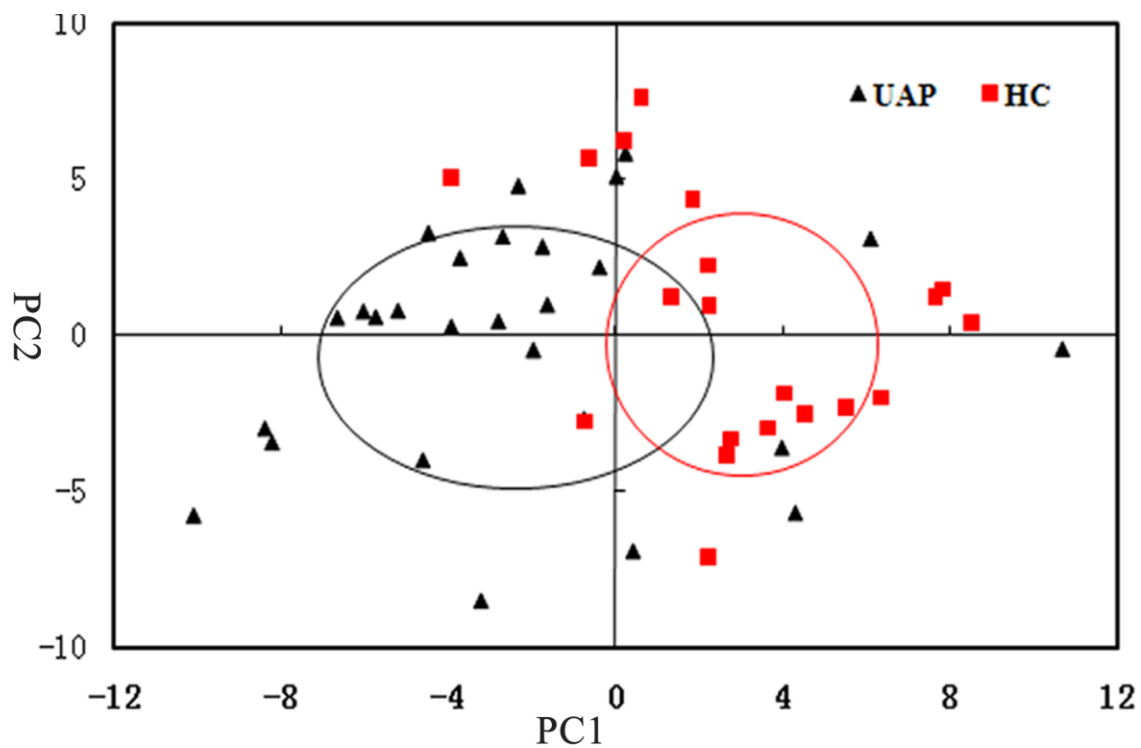
Figure 2. PCA score plot (PC1 *VS* PC2)of UAP patients and healthy controls (HC), Score plots showing discrimination between UAP (black triangles) and HC (red squares)(R2X = 68.1%, Q2 =25.1%)
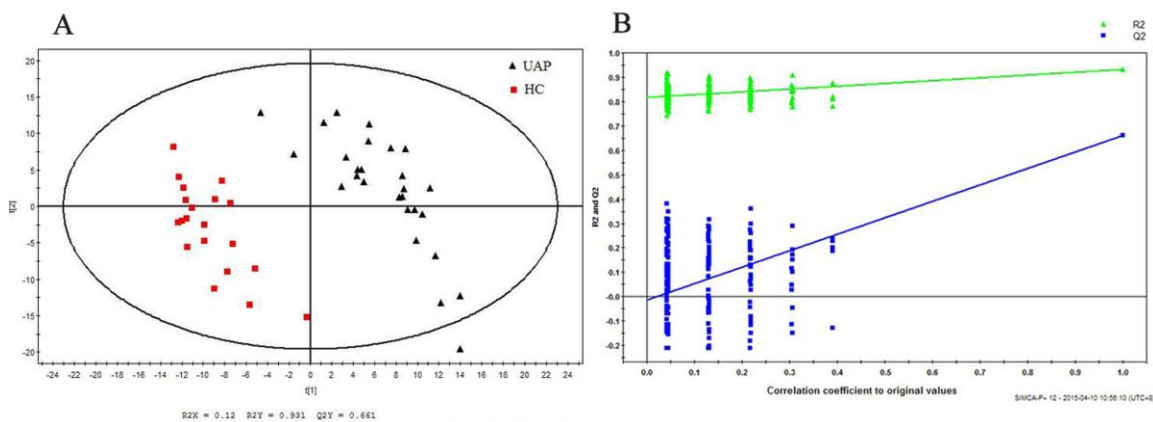
Figure 3. PLS-DA score plot(A) of UAP patients and healthy controls(HC), Score plots showing the degree of separation of the model between UAP (black triangles) and HC (red squares)(R2X = 12.1%, R2Y = 93.1%, and Q2 = 66.1%) and Statistical validation of the PLS-DA(B). A permutation test performed with 200 random permutations in a PLS-DA model showing R2 (green triangles) and Q2 (blue boxes) values from the permuted analysis (bottom left) significantly lower than the corresponding original values (top right).
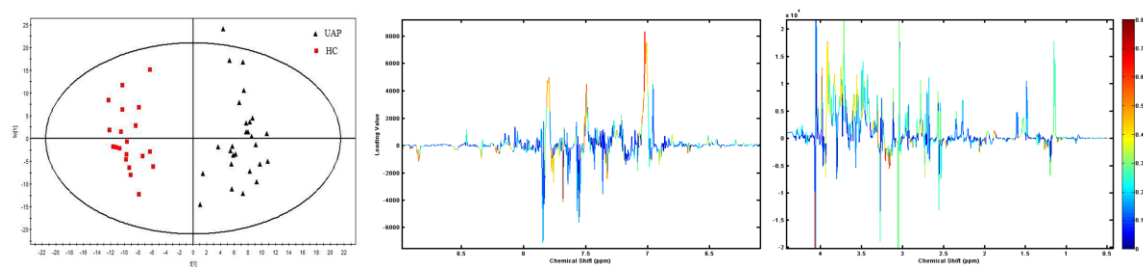
Figure 4. OPLS-DA score plot(A) of UAP patients and healthy controls(HC), Score plots displaying the degree of separation of the model between UAP (black triangles) and HC (red squares)(R2X = 12.1%, R2Y = 93.1%, and Q2 = 65.3%) and OPLS-DA Corresponding color-coded correlation coefficient loading plots (B) of key metabolites, demonstrating discrimination of key metabolite levels between UAP patients and healthy controls.
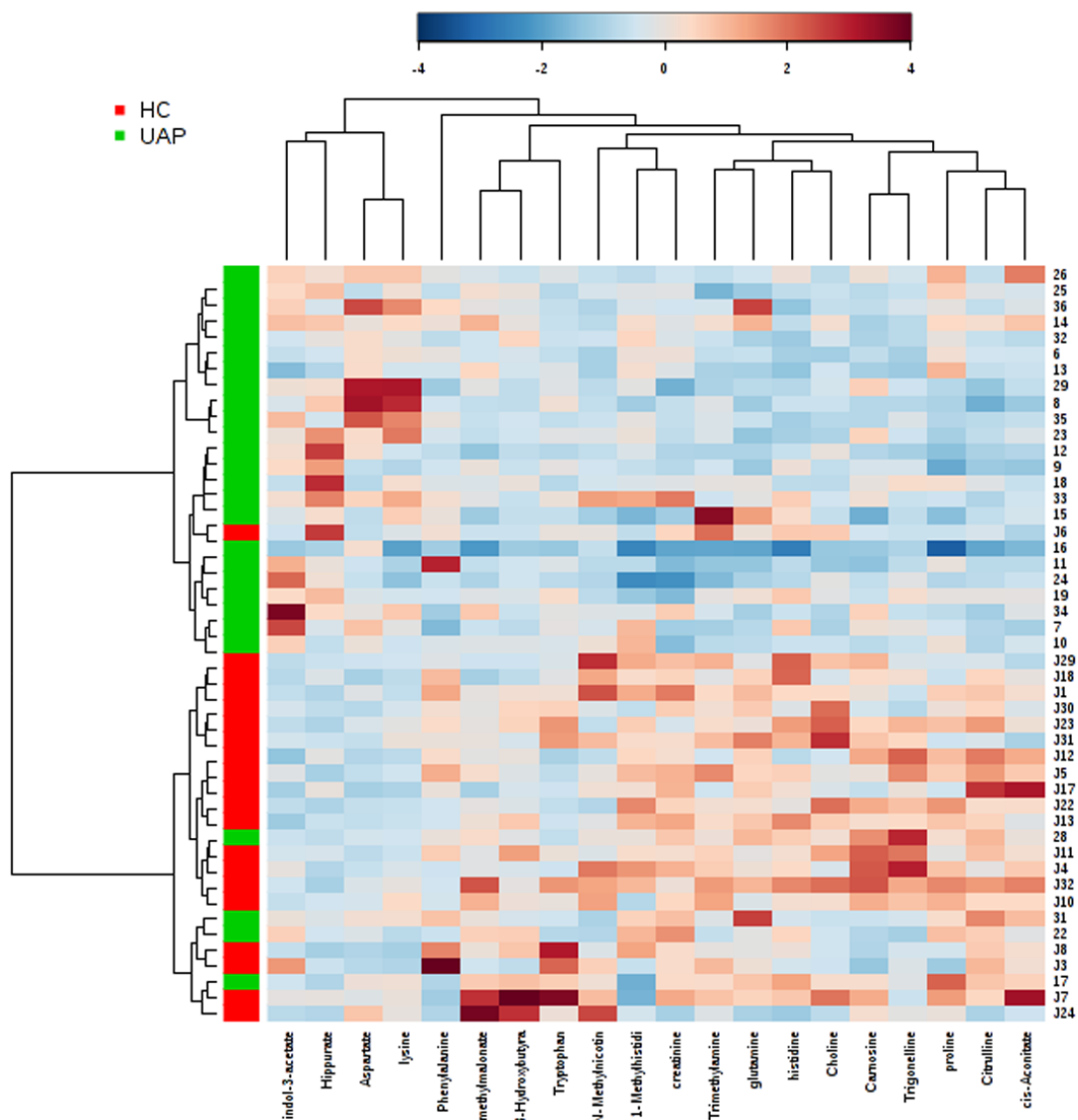
Figure 5. Heatmap visualization constructed based on 20 biomarkers implemented in MetaboAnalyst2.0. Rows: samples; columns: biomarkers. Green: UAP patients; red: healthy controls. Color key indicates metabolite expression value: dark blue: lowest; dark red: highest.
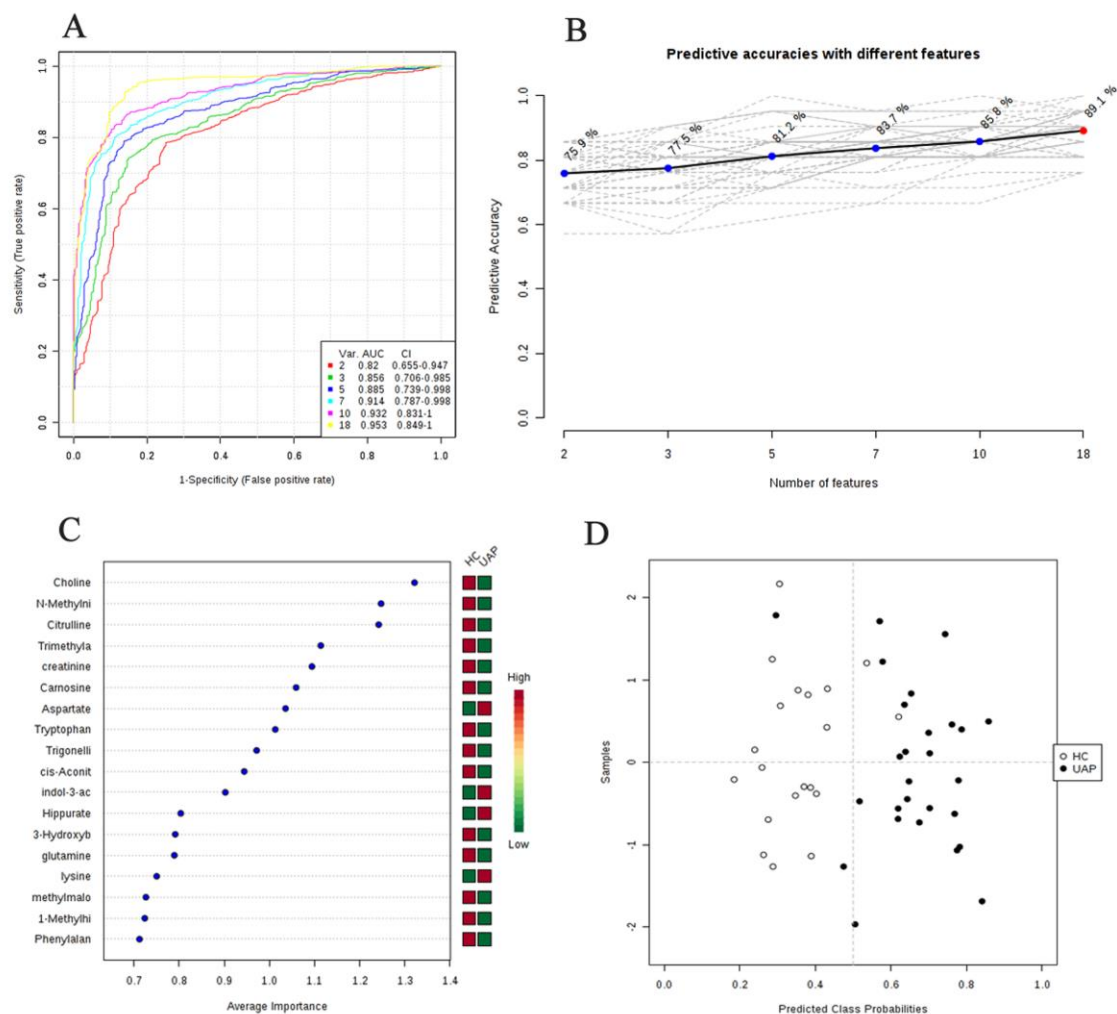
Figure 6. Comparison of different variables based on ROC curves (A),the legend shows the feature numbers and the AUCs of the six models, the predictive accuracies(B) with different features based on ROC curves, the average importance(C) of the 18 metabolites based on ROC curves, Variable Importance in Projection (VIP) plot indicating the most discriminating metabolite in descending order of importance, and (D)Prediction of UAP patients and control using MCCV analysis. The class membership of the left-out sample was predicted using an a priori cut-off value of 0.5 (dashed line).
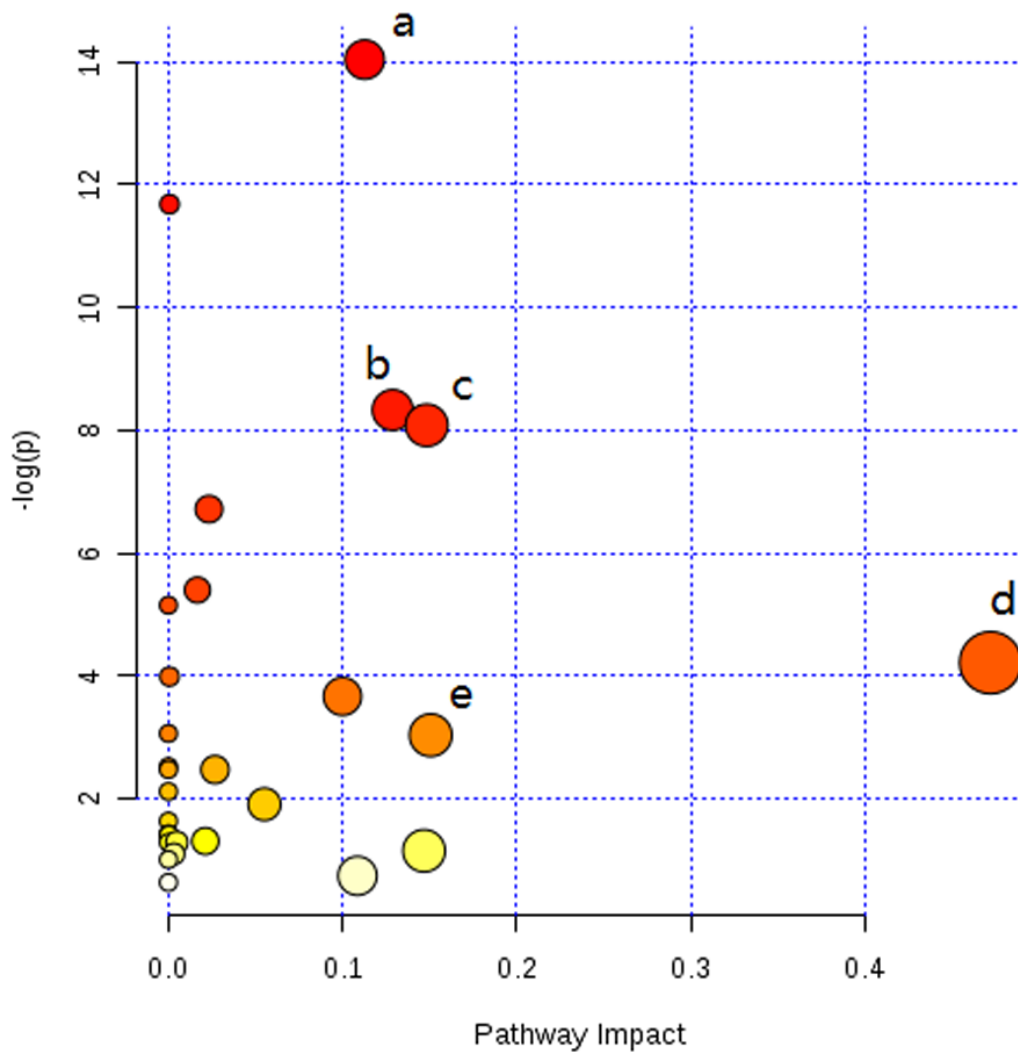
Figure 7. Summary of pathway analysis with MetPA (a) Aminoacyl-tRNA biosynthesis,

(b) Arginine and proline metabolism, (c) Histidine metabolism, (d) Alanine, aspartate and

glutamate metabolism, (e) Phenylalanine metabolism.

Table 1 Characteristics of UAP Patients and Healthy Controls

	patients	controls
total individuals (n)	27	20
age (years), range	62±5.98, 35-75	57.63±3.84,42-65
sex (F/M)	14/13	11/9
BMI	23.1±2.6,	24±4
Smoker (Y/N)	10/17	5/15
Triglycerides(mmol/L)	1.91±1.10	0.84±0.24
Cholesterol(mmol/L)	4.55±1.04	3.87±0.86
HDL(mmol/L)	1.11±0.27	1.23±0.31
LDL(mmol/L)	3.02±0.86	2.35±0.51
Use of antiplatelet drugs	27 (100%)	N/A
Use of nitrate esters drugs	12 (44.4%)	N/A
Use of statins	19 (70.3%)	N/A
Use of ACEI/ARB	2(7.4%)	N/A
Use of beta blocker	16 (59.3%)	N/A
Use of calcium channel antagonist	27 (100%)	N/A

Data are presented as mean ± SD. There was no significant difference in demographic data between

control and UAP patients.

Table 2 Quantitative comparison of metabolites found in urine of UAP patients and healthy controls

metabolites	Chemical shift	HMDB ID	Integral in UAP group[a] (mean ± std)×10^{-2}	Integral in HC group [a] (mean ± std)×10^{-2}	r [b] (|r|>= 0.432)	VIP	p[c] (p < 0.05)
3-hydroxybutyrate	**1.21(d)**, 2.32(m), 2.41(m)	HMDB00357	4.48 ± 1.74	7.32± 5.37	0.433 (↓)	1.96	0.03
methylmalonate	**1.25(d)**, 3.18(m)	HMDB00202	5.19 ± 1.31	6.26 ± 2.41	0.450 (↓)	2.05	0.05
lysine	1.74(m), **3.04(t)**, 3.77(t)	HMDB00182	3.93 ± 1.24	3.22 ± 0.40	0.439 (↑)	1.62	0.009
proline	2.03(m), 2.36(m), **3.43(m)**	HMDB00162	11.54 ± 2.85	13.08 ± 2.18	0.482 (↓)	1.98	0.05
glutamine	2.14(m), 2.46(m), **3.79(m)**	HMDB00641	6.74 ± 2.71	8.24 ± 1.38	0.498 (↓)	2.14	0.03
trimethylamine	**2.91(s)**	HMDB00906	2.97 ± 1.20	4.22 ± 0.86	0.461 (↓)	2.17	0.002
creatinine	**3.05(s)**, 4.07(s)	HMDB00562	357.6 ± 136.1	493.9 ± 84.3	0.587 (↓)	2.28	0.003
cis-aconitate	**3.12(s)**, 5.71(s)	HMDB00072	7.70 ± 3.24	11.31 ± 5.32	0.518 (↓)	2.36	0.006
citrulline	3.15(m), **3.77(t)**, 1.88(m)	HMDB00904	10.19 ± 3.73	15.51 ± 4.0	0.638 (↓)	2.63	0.003
histidine	3.14(m), **3.26(m)**, 7.11(s)	HMDB00177	12.06 ± 2.86	15.35 ± 3.04	0.579 (↓)	2.27	0.001
Choline	**3.21(s)**, 3.53(m), 4.08(m)	HMDB00097	10.10 ± 2.59	17.82 ± 7.03	0.621 (↓)	2.87	0.001
tryptophan	3.32(m), 3.50(m), **4.07(m)**	HMDB00929	6.73 ± 1.74	10.44 ± 5.44	0.493 (↓)	2.27	0.008
aspartate	2.69(m), 2.82(m), **3.91(m)**	HMDB00191	21.25 ± 8.95	13.67 ± 3.25	0.466 (↑)	1.86	0.001
hippurate	3.98(d), **7.54(t)**, 7.65(t)	HMDB00714	36.23 ± 18.42	22.44 ± 14.55	0.481 (↑)	2.47	0.008
indol-3-acetate	**7.17(t)**, 7.26(m), 7.52(d)	HMDB29738	2.27 ± 1.20	1.34 ± 0.62	0.461 (↑)	2.04	0.001
phenylalanine	**7.33(d)**, 7.39(t)	HMDB00159	5.52 ± 2.56	7.33 ± 3.48	0.453 (↓)	1.71	0.05
τ-methylhistidine	3.70(s), **7.02(s)**, 7.66(s)	HMDB00479	9.84 ± 2.73	11.70 ± 2.55	0.500 (↓)	1.86	0.02
carnosine	7.10(s), **8.12(s)**	HMDB00033	0.52 ± 0.30	0.93 ± 0.43	0.533 (↓)	2.25	0.001
N-methylnicotinamide	**8.19(t)**, 8.91(d), 8.98(d)	HMDB00699	0.74 ± 0.54	1.97 ± 1.19	0.713 (↓)	3.41	0.001
trigonelline	4.45(s), 8.85(m), **9.13(s)**	HMDB00875	0.65 ± 0.69	1.48 ± 0.94	0.503 (↓)	1.98	0.002

[a] the relative integrals of metabolites were determined from 1D ^{1}H NMR analysis of urine of each group. [b] The values of correlation number extracted from the correlation plots of OPLS-DA models. The cutoff values are 0.432 in the correlation-loading plot of UAP vs HC. [c] The p values were obtained from student's t-test. The chemical shifts in boldface were that we used in calculating integrals and p values. The arrows (↑/↓) were used to show the metabolite levels increase/ decreased compared with healthy controls.